symmetry

MDPI

Article

Lorenz Type Behaviors in the Dynamics of Laser Produced Plasma

Stefan Andrei Irimiciuc [1,2,*], Florin Enescu [3], Andrei Agop [4] and Maricel Agop [5,*]

1 National Institute for Laser, Plasma and Radiation Physics, 409 Atomistilor Street, Magurele, 077125 Ilfov, Romania
2 Institute of Physics of the Czech Academy of Sciences, Na Slovance 1991/2, 118 00 Prague, Czech Republic
3 Faculty of Physics, "Alexandru Ioan Cuza" University of Iasi, 700506 Iasi, Romania
4 Material Science and Engineering Department, "Gheorghe Asachi" Technical University of Iasi Romania, 700050 Iasi, Romania
5 Department of Physics, "Gh. Asachi" Technical University of Iasi, 700050 Iasi, Romania
* Correspondence: stefan.irimiciuc@inflpr.ro (S.A.I.); m.agop@tuiasi.ro (M.A.)

Received: 23 July 2019; Accepted: 4 September 2019; Published: 6 September 2019

Abstract: An innovative theoretical model is developed on the backbone of a classical Lorenz system. A mathematical representation of a differential Lorenz system is transposed into a fractal space and reduced to an integral form. In such a conjecture, the Lorenz variables will operate simultaneously on two manifolds, generating two transformation groups, one corresponding to the space coordinates transformation and another one to the scale resolution transformation. Since these groups are isomorphs various types isometries become functional. The Lorenz system was further adapted to describe the dynamics of ejected particles as a result of laser matter interaction in a fractal paradigm. The simulations were focused on the dynamics of charged particles, and showcase the presence of current oscillations, a heterogenous velocity distribution and multi-structuring at different interaction scales. The theoretical predictions were compared with the experimental data acquired with noninvasive diagnostic techniques. The experimental data confirm the multi-structure scenario and the oscillatory behavior predicted by the mathematical model.

Keywords: Lorenz system; fractal analysis; laser produced plasmas; plasma structuring; ionic oscillations

1. Introduction

Laser ablation embodies a series of phenomena with a complex interconnection between them [1]. For the better understanding of this physical process there have been multiple diagnostics techniques implemented which showcased the particle removal process [2], particle dynamics after ejection [3], plasma formation and expansion [4–6], etc. Complementary, theoretical aspects of the process have been steadily showcased in the past 30 years [7–9]. The difficulty in developing theoretical models for a multi-physics process like laser ablation comes from the combination of different elements from laser physics, solid state physics and plasma physics. Thus, an appropriate theoretical approach should be able to transition different interaction scale (ns or fs for the laser beam, fs or ps for the laser matter interaction and microsecond for the plasma expansion) and still keep a connective link between them.

The development of theoretical models that can accurately describe the ablation process has been a main direction for the understanding the underline phenomena and their interdependencies. A robust model needs to contain as input variables, laser properties, the nature of the material, ejection of the material and formation of a transient plasma. This is a difficult task as the majority of the existent theoretical approaches focus on particular sequences of the laser ablation. Therefore, we found classical theoretical approach that focused on ultra-short laser interaction with dielectric material or

metals [10], ns-laser ablation [11], thermal evaporation of material, particle ejection mechanisms and plasma formation or expansion. In the past decade there have been some proposals based on a fractal paradigm [12–14]. These attempts were focused on the behavior of the laser produced plasma, mainly on peculiar results like multiple structuring during expansion [6], particle oscillations [5] and temporal and spatial distribution of some plasma parameters [13]. The advantage of representing the laser ablation process in a multifractal space is given by the ease with which we can transition between different interaction scales and different sequences of the process. This was shown for a laser produced plasma on a single element [13] and multi-component target [12]. The core premise of the model is a hydrodynamic description of the plasma plume expansion, without an explicit involvement of the experimental parameters.

In this paper we develop a mathematical model starting from classic Lorenz system and we transpose it in nondifferential (fractal) representation. From such a perspective, Lorenz type variable will depend both on space coordinates and scale resolutions. Consequently, every variable will act as a limit of a family of functions which are non-differentiable for null scale resolutions and differentiable for non-null scale resolutions; every variable will operate simultaneously on two manifolds, one generated by the space coordinates' transformation group and another one generated by the scale resolution transformation group; these two groups are isomorphs, so that various types of isometries can be applied (embeddings, compactizations, etc.). The system will be solved in a fractal space. The final aim of this development is the understanding the dynamics of a laser produced plasma with a multi-component structure, generated on a complex target. The solution allows the simulation of particle velocity distribution across a wide range of scale resolutions; the charge particle spatial distribution, showcasing the formation of a space charge double layer at the interface between plasma structure; and charged current temporal trances at various scale resolutions. The theoretical predictions are compared with experimental data extracted from a laser produced plasma on a chalcopyrite target by means of Intensified Coupled Charged Device (ICCD) fast camera imaging and optical emission spectroscopy. The theoretical simulations are confirmed by the experimental data.

2. Mathematical Model

2.1. Route to Non-Differentiability

Non-linearity and chaoticity are fundamental attributes of a Lorenz type system. Usually, the classical models built to describe the Lorenz type dynamics, are developed on the presumption of differentiability and integrability at all scale resolutions. The successes of these approaches need to be understood sequentially, on domains in which the differentiability and integrability are still respected. The differential and integral mathematical procedures fail when we attempt to describe nondifferentiable dynamics of Lorenz type system.

In order to describe the non-differentiable dynamics of a Lorenz type system and attempt to remain tributary to the well-established differentiable and integral mathematical procedures, it is necessary to introduce the scale resolution both in the variable and differentiable equations describing such dynamics. All the variables are describing a Lorenz type system from a non-differentiable perspective, which depends on both space-time coordinates and the scale resolution. Consequently, instead of operating, for example, with a single variable described by a nondifferentiable function, we will operate only with the approximations of this function obtained by mediating it at various resolution scales. This special function will act as a limit of a family of functions which are non-differentiable for zero scale resolution and differentiable for non-zero scale resolutions.

This way of describing nondifferentiable dynamics of a Lorenz type system implies both the generation of a new geometry of movement and a new class of Lorenz type models (which we will refer to as fractal/multifractal Lorenz systems). According to these geometric studies for which the movement laws, invariants of the space time coordinates' transformation are integrated over the scale resolutions which are invariant of the scale resolution's transformation. If we further admit

that these geometric structures are based on the concept of multifractality, then the holographic implementation of movement—seen through scale relativity theory with an arbitrary fractal dimension or through operational procedures in the description of physical systems [14]-becomes essential when describing the dynamics of non-differentiable Lorenz type systems. However, both ways presented above imply the definition of nondifferentiable dynamics of a Lorenz type system on continuous but nondifferentiable curves. Therefore:

(i) Any variable used to describe the dynamics of a nondifferential Lorenz type system will be described through multifractal mathematical functions dependent on both the spatial and temporal coordinates, and on the scale resolution.
(ii) The laws describing these dynamics are invariant with respect to the spatial coordinates and temporal transformation, and the scale resolution transformation.
(iii) The constraints on the Lorenz type system dynamics, described through continuous and differentiable curves of a Euclidian space, are replaced by the dynamics of a system lacking any constraints, and being described by continuous and nondifferentiable curves in a multifractal space.
(iv) Between any two points in the multifractal space there is an infinity of curves describing the dynamics of a systems (its geodesics). The indiscernibility between these curves is a natural property of multifractalization through stochasticization; meanwhile, their discernibility is the result of a selection process based on the principle of maximum informational energy [14]. From such a perspective, any Lorenz type system with dynamics described by continuous and differentiable curves has hidden dissipative information (lacks memory). Otherwise, Lorenz type systems described by continuous and nondifferentiable curves have explicit information (presents memory).

Scale Resolutions

Let us consider a multifractal function (representing any of the variables describing the dynamics of a Lorenz type system) $f(u)$, defined in the closed interval $u \in [a, b]$. Let us also consider the set of values for the u variable:

$$u_a = u_0,\ u_1 = u_0 + \mu, \ldots,\ u_n + n\mu = u_b. \tag{1}$$

We will define $f(u, \mu)$ as the broken line connecting the points:

$$f(u_0),\ f(u_1), \ldots,\ f(u_n). \tag{2}$$

Then $f(u, \mu)$ becomes a μ-scale approximation.

Let us now consider $f(u, \overline{\mu})$, the $\overline{\mu}$-scale approximation of the same multifractal function. Since $f(u)$ is self-similar virtually everywhere, if $\overline{\mu}$ and μ are considered small, the approximations $f(u, \overline{\mu})$ and $f(u, \mu)$ lead to the same result when multifractal phenomena are investigated. Comparing these two situations, there is an infinitesimal increase/decrease $d\mu$ of μ that would correspond to an increase/decrease $d\overline{\mu}$ of $\overline{\mu}$, only in the case of scale contraction or dilatation. In that case, the following relationship is satisfied:

$$\frac{d\mu}{\mu} = \frac{d\overline{\mu}}{\overline{\mu}} = d\rho. \tag{3}$$

Therefore, the rational for the scale $\mu + d\mu$ and $d\mu$ needs to be constant. In these conditions we can consider the infinitesimal transformation of the scale as:

$$\mu' = \mu + d\mu = \mu + \mu d\rho. \tag{4}$$

by performing such a transformation, in the case of $f(u, \mu)$, it results in:

$$f(u, \mu') = f(u, \mu + \mu d\rho). \tag{5}$$

Furthermore, if we use stop at the first approximation of the function we get:

$$f(u,\mu') = f(u,\mu) + \frac{\partial f}{\partial \mu}(\mu' - \mu). \tag{6}$$

Meaning,

$$f(u,\mu') = f(u,\mu) + \frac{\partial f}{\partial \mu}\mu d\rho. \tag{7}$$

Moreover, we note that, for a fixed arbitrary μ_0,

$$\frac{\partial ln\frac{\mu}{\mu_0}}{\partial \mu} = \frac{\partial(ln\mu - ln\mu_0)}{\partial \mu} = \frac{1}{\mu}, \tag{8}$$

so that Equation (7) can be rewritten as:

$$f(u,\mu') = f(u,\mu) = \frac{\partial f(u,\mu)}{\partial \ln\left(\frac{\mu}{\mu_0}\right)} d\rho. \tag{9}$$

In the end we will obtain:

$$f(u,\mu') = \left[1 + \frac{\partial}{\partial \ln\left(\frac{\mu}{\mu_0}\right)} d\rho\right] f(u,\mu). \tag{10}$$

which showcases the dilatation/contraction operator:

$$\hat{O} = \frac{\partial}{\partial \ln\left(\frac{\mu}{\mu_0}\right)}. \tag{11}$$

Equation (11) also showcases the fact that the intrinsic variation of the scale resolution is not in μ but on $\ln\left(\frac{\mu}{\mu_0}\right)$.

2.2. Non-Differentiable Lorenz Type Systems

Let us now consider the classic Lorenz system [15,16] described in a non-dimensional coordinate system by the differentiable equations:

$$\begin{aligned} \frac{d\overline{X}}{d\overline{T}} &= \sigma\left(\overline{X} - \overline{Y}\right). \\ \frac{d\overline{Y}}{d\overline{T}} &= -r\overline{X} - \overline{Y} - \overline{XZ}. \\ \frac{d\overline{Z}}{d\overline{T}} &= -b\overline{Z} + \overline{YX}. \end{aligned} \tag{12}$$

In Equation (12) the variables are obviously differentiable and can be integrated. According to the paradigm presented above, when we consider the non-differentiable and non-integrable variables, the system of Equation (12) becomes a multifractal Lorenz type system. For this to occur, the variable needs to be dependent both on the spatial and temporal coordinates, and on the scale resolution. Moreover, the affine parameter $\overline{T}$ which characterizes the trajectories in the space phase ($\overline{X}$, $\overline{Y}$ and $\overline{Z}$) needs to be dependent on the resolution scale. Using such a hypothesis, the variables $\overline{X}$, $\overline{Y}$ and $\overline{Z}$ will operate

simultaneously on two manifolds, one generated by the space-time coordinates' transformation group and another one generated by the scale resolution transformation group. Since these two group are isomorphs, or in an extremely restrictive case self-morphs, embedding type isometries, self-embedding isometries, compactization type isometries, etc., become functional.

A possible embedding scenario can be performed through scaling:

$$\overline{X} \to \frac{X}{\varepsilon},\ \ \overline{Y} = \frac{Y}{\sigma\varepsilon^2}, \overline{Z} = \frac{Z}{\sigma\varepsilon^2}, \overline{T} = \varepsilon T. \tag{13}$$

with,

$$\varepsilon = ln\frac{\mu}{\mu_0}. \tag{14}$$

In Equations (13) and (14), ε can functionally be dependent on only one fractal dimension, D_F, following the relationship $\varepsilon = \varepsilon(D_F)$. In that case, using Equation (12) we will describe the dynamics of a mono-fractal Lorenz type system. We can find another case of ε which can be dependent on a singularity spectrum f_α following the relationship $\varepsilon = \varepsilon(f_\alpha)$. In that case, Equation (12) describes the dynamics of a multifractal Lorenz type system.

The scaling Equation (13) specifies the fact that, simultaneously with the contraction in the space phase attributed to a mono-fractal or multifractal dynamics of a Lorenz type system, the dilation of time takes place. As such, the classical Lorenz system (12) through (13) and (14) becomes a multifractal Lorenz type system described by the following system:

$$\begin{aligned} \frac{dX}{dT} &= Y - \varepsilon\sigma X. \\ \frac{dY}{dT} &= X - \varepsilon Y - XZ. \\ \frac{dZ}{dT} &= XY - \varepsilon bZ. \end{aligned} \tag{15}$$

either through $\varepsilon = \varepsilon(D_F)$ or $\varepsilon = \varepsilon(f_\alpha)$.

In this system the dynamics variables X, Y and Z are multi fractal functions, as they depend not only on the space-time coordinates but also on the scale resolution. Therefore, instead of working with X, Y and Z variables, which are described by non-differentiable functions, we will operate only with approximations of these functions obtained by their averaging at various scale resolutions given by Equation (14). Any of the variables X, Y or Z will behave like limits of a family of functions, which are non-differentiable on null scale resolutions ($\varepsilon \to 0$, and $\mu = \mu_0$) and differentiable on nonzero scale resolutions ($\varepsilon \neq 0$). In these conditions the movement laws given by Equation (15), regardless of any coordinate transformations, can be integrated with the scale laws, regardless of any scale resolution transformations.

In such context, a further in-depth study of the systems dynamics needs to be done for the case in which the scale resolution is null, thus for the case in which Equation (15) defines a non-differential system. Let us consider that in Equation (15) the scale resolution in null, thus the restriction $\varepsilon \to 0$ is satisfied. Then Equation (15) takes the following form:

$$\begin{aligned} \frac{dX}{dT} &= Y. \\ \frac{dY}{dT} &= X - XZ. \\ \frac{dZ}{dT} &= XY. \end{aligned} \tag{16}$$

2.3. Motion Integration

The system in Equation (16) presents some interesting features, such as the phase space volume associated to the dynamics of the system being conserved, since it satisfies the relationship:

$$\frac{\partial}{\partial X}\left(\frac{\partial X}{\partial T}\right)+\frac{\partial}{\partial Y}\left(\frac{\partial Y}{\partial T}\right)+\frac{\partial}{\partial Z}\left(\frac{\partial Z}{\partial T}\right)=0 \tag{17}$$

This means that through the restriction $\varepsilon \to 0$, describing the transition from a differentiable Lorenz type system to a non-differentiable Lorenz type system, the system evolves from a dissipative one to a non-dissipative one. The non-differentiable Lorenz type system admits two integrals of the motions. The first is:

$$\frac{X^2}{2}-Z=k_1=const. \tag{18}$$

This relation is obtained by multiplying the first equation from (16) with Y and further substituting the term XY through the third equation of Equation (16) and finally integrating the result. The second movement's integral is:

$$\frac{1}{2}Y^2-Z+\frac{1}{2}Z^2=k_2=const. \tag{19}$$

Relation (19) is achieved by multiplying the second equation from Equation (16) with Y, substituting the terms XY and XYZ with the third equation from Equation (16), and finally integrating the result. Let us further note that the dynamics introduced through a non-differential Lorenz type system are described analytically through elliptic functions. In order to showcase this, let us consider the square of Equation (16) using Equations (18) and (19), written as:

$$\dot{X}^2=Y^2=2k_2+2Z-Z^2=2k_2+\left(X^2-2k_1\right)-\left(\frac{1}{2}X^2-k_1\right)^2. \tag{20}$$

It reveals the elliptic integral:

$$\int\frac{dX}{\sqrt{P(X)}}=\frac{1}{2}\int dT. \tag{21}$$

with

$$P(X)=-X^4+4X^2(1+k_1)+4\left[2(k_2-k_1)-{k_1}^2\right]. \tag{22}$$

Admitting that the $P(X)$ polynom can be written as:

$$P(X)=\left(u_1^2-X^2\right)\left(X^2-u_2^2\right),$$

where u_1^2 and u_2^2 have the following expressions:

$$u_{1,2}^2=2\left[(1+k_1)\pm(1+2k_2)^{1/2}\right]. \tag{23}$$

The integral (21) becomes:

$$\int\frac{dX}{\left[\sqrt{\left(u_1^2-X^2\right)\left(u_2^2-X^2\right)}\right]}=\frac{i}{2}\int dT. \tag{24}$$

Furthermore, by using the substitutions:

$$w=\frac{X}{u_2},\ s=\frac{u_2}{u_1} \tag{25}$$

the integral (24) takes the Legendre form:

$$\frac{dw}{\sqrt{(1-w^2)(1-s^2w^2)}} = \frac{iu_1}{2}\int dT. \tag{26}$$

The solution to that integral is the Jacobi elliptic function *sn*,

$$w = sn\left[\frac{iu_1}{2}(\Delta T); s\right] \tag{27}$$

or in its original coordinates:

$$X = u_2 sn\left[\frac{iu_1}{2}(\Delta T); s\right]. \tag{28}$$

From here, through Equation (18) we will get the expression for Z:

$$Z = \frac{{u_2}^2}{2} sn^2\left[\frac{iu_1}{2}(\Delta T); s\right] - k_1. \tag{29}$$

while by using Equation (19) we can obtain the expression for Y:

$$Y_{1,2} = \pm\left\{2(k_2-k_1) + k_1^2 + u_2^2(1+k_1)sn^2\left[\frac{iu_1}{2}(\Delta T); s\right] - \frac{u_2^4}{4}sn^4\left[\frac{iu_1}{4}(\Delta T); s\right]\right\}^{1/2}. \tag{30}$$

Now, the expressions for X, Y and Z can be simplified even more if we take into account the relationship:

$$sn\left[\frac{iu_1}{2}(T-T_0); s\right] = i\frac{sn\left[\frac{iu_1}{2}(\Delta T); s'\right]}{cn\left[\frac{iu_1}{2}(\Delta T); s'\right]}. \tag{31}$$

cn is a Jacobi elliptical function, s is the modulus of the elliptical functions *cn* and *sn* and s' is the complementary modulus ${s'}^2 = 1 - s^2$a and $\Delta T = T - T_0$.

In the following we will attempt to implement the solution gained by Lorenz system to a well-known system covering the ejection and dynamics of particles.

3. Plasma Modelling

The fractal representation of phenomena like laser produced plasma has a simplified elegance, as it confines all the complex intricate behaviors in a handful of parameters. This is a great advantage when attempting to simulate a wide range of behaviors for multiple external conditions, spatial and temporal coordinates, etc. However, the interpretation of the obtained results requires a direct correspondence between the compact fractal parameters and real, measurable plasma parameters. Given the description of our three normalized functions (X, Y and Z) they define complex functions that will be used further to describe formation and evolution of the ejected particles at different scale resolutions. Therefore, in our paradigm: X will define the particle distributions, Y will define the charged particle current as a function and Z will define the charge density fluctuations induced by some unbalances of the transient electrical field during expansion, and can be associated with the ratio between the kinetic and thermal energy of the ejected particles. Let us note that we will operate with the previous functions and parameters as normalized quantities. Since the Laser Produced Plasmas (LPP) dynamics are described through continuous and non-differentiable curves (fractal curves with different degrees of fractality), we had to operate in this situation with what we call the singularity spectrum. If in the system the dynamics are characterized by only one fractal dimension then we are dealing with mono fractal dynamics. If for a system (which is the case for laser produced plasmas) we deal with simultaneous dynamics with various fractal dimensions, then the role of the singularity

spectra is not only to showcase the variation domain of these dimensions but also the characteristic classes associated by defining the strange attractors.

In Figure 1a,b we have represented the particle velocity distribution at various scale resolutions and at various moments in time. We can see from the two representations that the evolution of the plasma in time, implies the presence of families of particles defined by specific scale resolutions and velocity distributions. With an increase of the scale resolution we see that the fractal image of the laser produced plasma showcases the appearance of a one particle distribution centered on a relatively high velocity, at low resolutions scale and a consistent increase number of distributions centered around lower velocities. The presence of multiple structures in laser produced plasma has been previously attested and reported as a direct result of the multiple ejection mechanism and plasma interaction with the background gas. We note that the presence of multiple ejection mechanisms [17–20] (Coulomb explosion, explosive boiling, phase explosion, etc.) will lead to the presence, within the plasma volume, of particles or plasma structure defined by different fractalization and scale resolutions. The simulations also showcase a transition from quasi mono-energetic particles ejected through a single ablation mechanism to an amalgam of particles with different energetic distributions specific to each ejection mechanism involved.

In Figure 1b we represented the particle distribution with the scale resolution for various moments in time. As the plasma evolves we see the presence of multiple distribution sites centered across low ($s < 0.3$) and high ($0.4 < s < 1$) resolution scales. This suggests that the first ejected particles ($\Delta T = 40$) are defined only by one scale resolution, characteristic of the Coulomb explosion mechanism. For longer period of time, when the thermal mechanism is dominant, we see multiple distributions centered on higher values of the scale resolutions. Therefore, our simulations capture the ejection of a series of particles with different kinetic energies and fractalizations. As such, we can now define a scale resolution for each of the ejection mechanisms (~ 0.2 for Coulomb Explosion, ~0.6 for Explosive Boiling and ~1 for the removal of complex structures) ensuring a wide covering of our theoretical model, transcending the Coulomb temporal scale, up to the explosive boiling ejection scenario and the ejection of clusters and more complex structures.

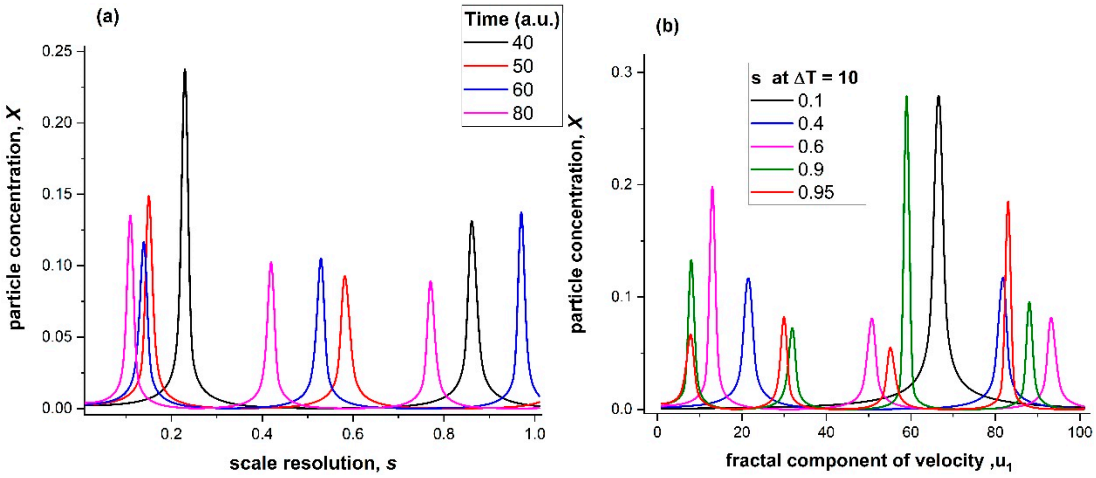

Figure 1. (**a**) Particle velocity distribution for various scale resolutions, (**b**) particle distribution with the scale resolution distribution at various moments in time.

In Figure 2a we have represented the charge density fluctuations induced by some unbalances with respect to the plasma volume (ξ). We can see that for short moments of time we observed a separation of the charges. The obtained distribution in the fractal space resembles the double layer distribution in the case of classical plasma physics [18]. As the time evolves, the double-layer-like distribution moves towards higher distances, and for longer moments of time a secondary one appears. This behavior is in line with the transient double layer scenario published by Bulgakova [20]. The charge

separation that occurs during the Coulomb explosion will act as a driving force behind the expansion of the particles. The double layer formed during the particle expansion will lead to the acceleration of ions and the deceleration of the electron. This exchange will induce some current oscillations [21] with the frequency depending of the nature of the material, and thus on its fractality. The formation of the second plasma structure, expanding with a lower velocity and being described as having a different temperature [22], will also lead to the formation of a double layer between the fast structure and slow structure [20]. This phenomenon was showcased by us in Figure 2a, where we can see the appearance of a second signature of the double layer in the charged particle distribution at a later evolution time. The intensity of the function represented in Figure 2a increases with the increase of time and we can see that at longer expansion time, where the formation of a second plasma structure becomes visible, another more intense double layer forms. This result was expected, as the multiple structures formed within the plasma volume suffered a spatial and temporal expansion. In order to maintain the composed global shape and to compensate the loses, particle density, with an increase in the separation between the two structures, of the electrical field defining the double layers increase their amplitudes. In Figure 2b, we have represented the particle current evolution in time for various scale resolutions. We noticed that the particles present an oscillatory dynamic, as was previously reported by [23] and experimentally proven in [24] and [25]. The frequency changes with the scale resolution, thus we deduce that each component of the plasma might present a different oscillatory behavior dictated by the characteristics of the double layer formed in the area separating the structures.

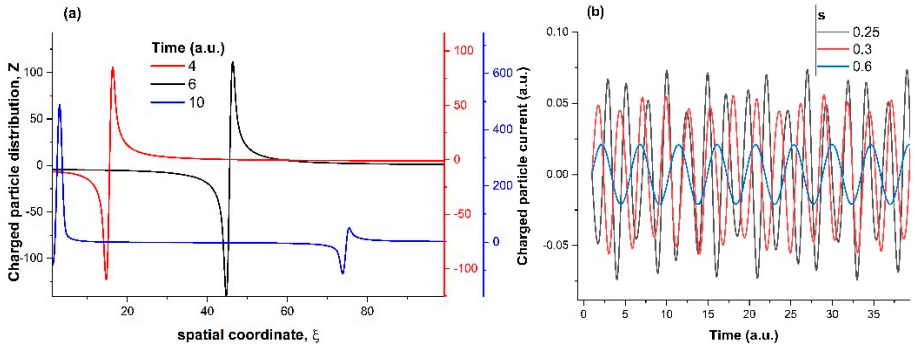

Figure 2. (**a**) Charged particles' distribution at various moments in time, (**b**) charge particle current induced by fluctuation current at the resolution scale.

4. Experimental Confirmation

In order to verify if our theoretical assumptions can have experimental correspondents we investigated by means of ICCD fast camera imaging and space-and-time-resolved optical emission spectroscopy of a plasma generated by an ns laser beam on a Chalcopyrite mineral target. The experiments were performed in fixed external conditions (laser fluence 5 J/cm^2 and background pressure of 10^{-2} Torr). The choice of the relatively simple mineral comes from its composition, having elements with different physical properties (S, Cu and Fe) which will allow a better showcase of phenomena like: particle separation, ionic oscillations and plume splitting. Further details on the experimental set-up can be found in [6,12].

In Figure 3a we have represented the spatial distribution of spectral region 420–430 nm after a time delay of 650 ns. This region is significative for our laser produced plasmas as it contains all the elements composing the target (Cu I-II, Fe I-II and S II). We noticed that the atomic emission lines can be found only for short distance while the ionic lines start and end emission at considerably longer distances. This result confirms other findings from literature and underlines the separation of the plasma components into fast and slow [26], respecting the ejection mechanism behind each species. In Figure 3b we have plotted the spatial distribution of representative emission lines for all the atomic and ionic species. Due to the difference in expansion velocities between ionic (S II-15.4 km/s,

Fe II-14.3 km/s and Cu II-11.4 km/s) and atomic species (Fe I-6.2 km/s and Cu I-4.4 km/s), the ions can be seen expanding at longer distances with respect to the target surface. The slightly increased velocity of S ions compared with Fe or Cu ones is a direct consequence of the acceleration in the double layer generated through Coulomb expansion [27]. We also notice periodic fluctuations (oscillations) on the spatial distribution of all the ionic species. The period of these oscillation are of approximately 900 kHz in good agreement with other reports of ionic oscillations in laser produced plasmas [21,24,28]. The first attempts for the comprehension of this "peculiar" behavior was based on the formation of single or multiple double-layers in the very vicinity of the target. This picture was the main focus to a long series of papers reporting on charge separation in laser-produced plasma, mainly from the 1980s [29,30]. Eliezer and Hora [23] gathered, in a very comprehensive manner, the state of the art regarding the double and multiple layers in laser-produced plasmas. One of the remarkable results reported are experimental proofs with double-layer electric fields of 105–106 V/cm and widths of 10–100 Debye lengths. In the past few years, three other theoretical approaches where proposed. One based on the fractal model developed as the interaction between two fractal structures [5,31], and their corresponding interface (generally, this interface delineates the double layer), with the second ones being on differential physics [28]: a collisional model based on the plasma ion frequency and electron-ion collision rate in the context of the Lieberman's model for plasma immersion ion implantation, and finally, one based on the AC Josephson effect. So, at this point there is no real consensus for the real mechanism behind the oscillatory behavior but intense theoretical and experimental work is undergoing to shed some light on it.

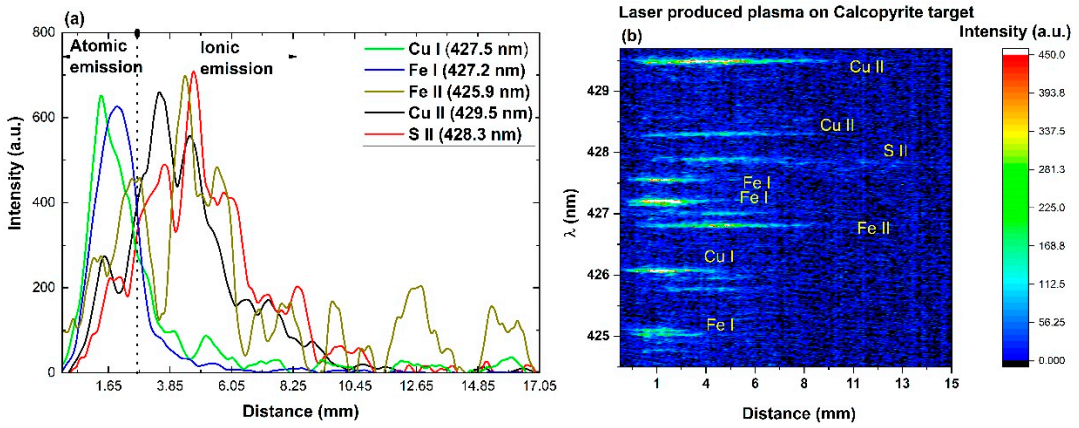

Figure 3. (**a**) Spatial mapping of Cu, S and Fe emission after 650 ns, (**b**) bi-dimensional representation of atomic and ionic emission.

To verify how the distribution of the compositional species within the plasma volume would affect the overall behavior of the laser produced plasma, we recorded the overall emission of the plasma at various moments in time. In Figure 4a we show a representative image of the plasma at a time-delay of 650 ns. If we perform cross section across the main expansion axis (centered around the orthogonal direction on the target in the impact point), three areas are more visible as the time delay increases. The first area seen at a larger distance corresponds to an ion rich area (confirmed by the data presented in Figure 3b) expanding with 16 km/s; the second one corresponds to an atomic rich area (~6 km/s); and the emission maxima corresponds to the maxima of the atomic emission. The last area has a small intensity and it is in the proximity of the target. It corresponds to the emission from atomic species colliding with clusters and microdroplets ejected from the target. This emission was not seen in the spectra's resolved measurements but remains a trademark of a strong thermal mechanism and the ejection of clusters and nanoparticles [32]. The difference in expansion velocity is a signature of the fundamental ejection mechanism behind each structure. The first structure contains mainly ions and it is induced during Coulomb explosion. The second structure contains mainly atomic species ejected by the thermal mechanism which require a longer incubation time (up to a few ns), thus displaying a

lower velocity. The third structure mainly contains nanostructures, or clusters ejected directly from the target and expanding with a significantly lower velocity (generally found in the order of hundreds of m/s).

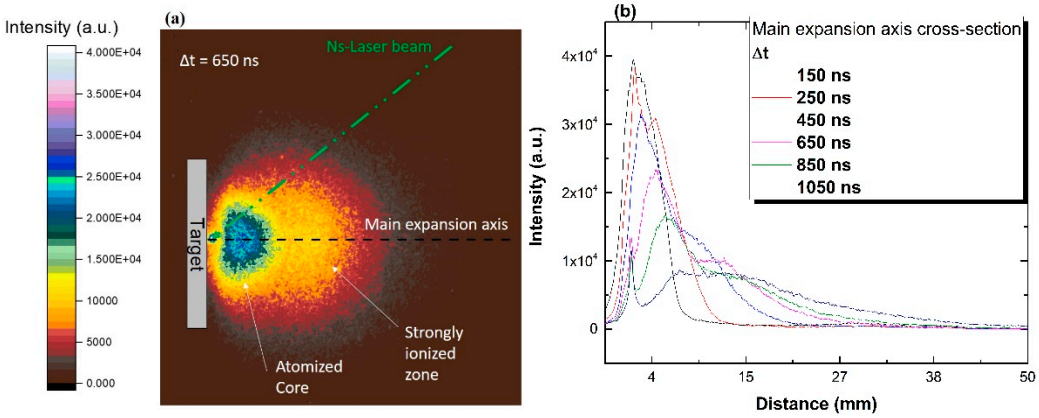

Figure 4. (**a**)ICCD fast camera image of a LPP Chalcopyrite collected after 650 ns, (**b**) cross section for a series of images extracted at various time delays.

The experimental data extracted from a plasma generated on chalcopyrite mineral by irradiation with an ns laser beam confirms the theoretical projections presented in Section 3. The temporal separation the plasma components based on their inner properties accurately reflects the separation based on the resolution scale of each type of ablation mechanism and the presence of multiple distribution on the scale resolution representation. One of the most important results is the prediction and confirmation of ionic oscillations by using invasive techniques. The oscillatory behavior coupled with heterogenic dynamics of different ions is well in line with the image depicted by other groups [20,33] and by our group in past papers [5,13,31]. In this paper the oscillatory behavior and the double layer-like distribution appear as natural solutions to the initial paradigm which translated the initial complex Lorenz system from laser to target to plasma. As such, we were able to build a robust theoretical model that can contains the set of parameters for the laser, target and the projection of the particle dynamic after ejection as solutions to the initial system.

5. Conclusions

A non-differential Lorenz system was built by projecting a differential Lorenz system on a fractal space. Simulations are performed for a wide range of scale resolutions showcasing the appearance of multiple distribution centered on different velocities attributed to the various plasma formed through different removal mechanisms. Current oscillations were also predicted as a result of the appearance of multiple double layers during expansion.

The theoretical simulations were confronted with experimental data extracted by means of ICCD fast camera imaging and space and time resolved optical emission spectroscopy of a complex plasma generated by ns-laser ablation on a chalcopyrite sample. Space and time resolved measurement revealed an oscillating behavior seen in the emission of the Cu, Fe and S ions. The ions were found to expand with various velocities specific to each species present in the plasma. The ICCD imaging revealed the split into two structures (fast and slow) expanding with different velocities. The values were found consistent with the ones of the individual species seen through spectrally resolved measurements. The experimental data is in good agreement with the major predictions made by the theoretical model based on the Lorenz system.

Author Contributions: Conceptualization, M.A. and S.A.I.; methodology, S.A.I., A.A. and M.A.; investigation, S.A.I., A.A and F.E; writing—original draft preparation, S.A.I. and M.A.; writing—review and editing, F.E. and A.A.; visualization, S.A.I.; supervision, M.A.

Funding: This work has been funded by the National Authority for Scientific Research and Innovation in the framework of the Nucleus Program—16N/2019.

Conflicts of Interest: The authors declare no conflict of interest. The funders had no role in the design of the study; in the collection, analyses, or interpretation of data; in the writing of the manuscript, or in the decision to publish the results.

References

1. Phipps, C.R. *Laser Ablation and Its Applications*; Springer Series in Optical Sciences; Springer: Boston, MA, USA, 2007; Volume 129, ISBN 978-0-387-30452-6.
2. Autrique, D.; Clair, G.; L'Hermite, D.; Alexiades, V.; Bogaerts, A.; Rethfeld, B. The role of mass removal mechanisms in the onset of ns-laser induced plasma formation. *J. Appl. Phys.* **2013**, *114*, 023301. [CrossRef]
3. Toftmann, B.; Schou, J. Time-resolved and integrated angular distributions of plume ions from silver at low and medium laser fluence. *Appl. Phys. A Mater. Sci. Process.* **2013**, *112*, 197–202. [CrossRef]
4. Geohegan, D.B.; Puretzeky, A.A.; Duscher, G.; Pennycook, S.J. Time-resolved imaging of gas phase nanoparticle synthesis by laser ablation. *Appl. Phys. Lett.* **1998**, *72*, 2987. [CrossRef]
5. Irimiciuc, S.A.; Mihaila, I.; Agop, M. Experimental and theoretical aspects of a laser produced plasma. *Phys. Plasmas* **2014**, *21*, 093509. [CrossRef]
6. Irimiciuc, S.A.; Bulai, G.; Gurlui, S.; Agop, M. On the separation of particle flow during pulse laser deposition of heterogeneous materials—A multi-fractal approach. *Powder Technol.* **2018**, *339*, 273–280. [CrossRef]
7. Anisimov, S.I.; Luk'yanchuk, B.S. Selected problems of laser ablation theory. *Phys.-Uspekhi* **2002**, *45*, 293–324. [CrossRef]
8. Bulgakova, N.M.; Stoian, R.; Rosenfeld, A.; Hertel, I.V.; Marine, W.; Campbell, E.E.B. A general continuum approach to describe fast electronic transport in pulsed laser irradiated materials: The problem of Coulomb explosion. *Appl. Phys. A Mater. Sci. Process.* **2005**, *81*, 345–356. [CrossRef]
9. Kelly, R.; Miotello, A. On the role of thermal processes in sputtering and composition changes due to ions or laser pulses. *Nucl. Instrum. Methods Phys. B* **1998**, *141*, 49–60. [CrossRef]
10. Bulgakova, N.M.; Stoian, R.; Rosenfeld, A.; Hertel, I.V. Continuum Models of Ultrashort Pulsed Laser Ablation. In *Laser-Surface Interactions for New Materials Production*; Miotello, A., Ossi, P., Eds.; Springer: Berlin/Heidelberg, Germany, 2010; Volume 130, pp. 81–97.
11. Autrique, D.; Chen, Z.; Alexiades, V.; Bogaerts, A.; Rethfeld, B. A multiphase model for pulsed ns-laser ablation of copper in an ambient gas. *AIP Conf. Proc.* **2012**, *1464*, 648–659.
12. Irimiciuc, S.; Bulai, G.; Agop, M.; Gurlui, S. Influence of laser-produced plasma parameters on the deposition process: In situ space- and time-resolved optical emission spectroscopy and fractal modeling approach. *Appl. Phys. A Mater. Sci. Process.* **2018**, *615*, 1–14. [CrossRef]
13. Irimiciuc, S.A.; Gurlui, S.; Nica, P.; Focsa, C.; Agop, M. A compact non-differential approach for modeling laser ablation plasma dynamics. *J. Appl. Phys.* **2017**, *121*, 083301. [CrossRef]
14. Merches, I.; Agop, M. *Differentiability and Fractality in Dynamics of Physical Systems*; World Scientific: Singapore, 2015; ISBN 978-981-4678-38-4.
15. Haken, H. *Synergetics*; Springer: Berlin, Germany, 1983; ISBN 978-3-642-88338-5.
16. Arfken, G.; Weber, H.; Harris, F.E. *Mathematical Methods for Physicsists*, 7th ed.; Academic Press: Cambridge, MA, USA, 2012; ISBN 9780123846556.
17. Dachraoui, H.; Husinsky, W.; Betz, G. Ultra-short laser ablation of metals and semiconductors: Evidence of ultra-fast Coulomb explosion. *Appl. Phys. A Mater. Sci. Process.* **2006**, *83*, 333–336. [CrossRef]
18. Kelly, R.; Miotello, A. Comments on explosive mechanisms of laser sputtering. *Appl. Surf. Sci.* **1996**, *96–98*, 205–215. [CrossRef]
19. Merino, M.; Ahedo, E. Two-dimensional quasi-double-layers in two-electron-temperature, current-free plasmas. *Phys. Plasmas* **2013**, *20*, 023502. [CrossRef]
20. Bulgakov, V.; Bulgakova, N.M. Dynamics of laser-induced plume expansion into an ambient gas during film deposition. *J. Phys. D Appl. Phys.* **1999**, *28*, 1710–1718. [CrossRef]

21. Focsa, C.; Gurlui, S.; Nica, P.; Agop, M.; Ziskind, M. Plume splitting and oscillatory behavior in transient plasmas generated by high-fluence laser ablation in vacuum. *Appl. Surf. Sci.* **2017**, *424*, 299–309. [CrossRef]
22. Jiang, L.; Tsai, H.-L. A plasma model combined with an improved two-temperature equation for ultrafast laser ablation of dielectrics. *J. Appl. Phys.* **2008**, *104*, 093101. [CrossRef]
23. Eliezer, S. Double layers in laser-produced plasmas. *Phys. Rep.* **1989**, *172*, 339–407. [CrossRef]
24. Singh, S.C.; Fallon, C.; Hayden, P.; Mujawar, M.; Yeates, P.; Costello, J.T. Ion flux enhancements and oscillations in spatially confined laser produced aluminum plasmas. *Phys. Plasmas* **2014**, *21*, 093113. [CrossRef]
25. Borowitz, J.L.; Eliezer, S.; Gazit, Y.; Givon, M.; Jackel, S.; Ludmirsky, A.; Salzmann, D.; Yarkoni, E.; Zigler, A.; Arad, B. Temporally resolved target potential measurements in laser-target interactions. *J. Phys. D Appl. Phys.* **1987**, *20*, 210–214. [CrossRef]
26. Irimiciuc, S.; Boidin, R.; Bulai, G.; Gurlui, S.; Nemec, P.; Nazabal, V.; Focsa, C. Laser ablation of (GeSe2)100−x(Sb2Se3)$_x$ chalcogenide glasses: Influence of the target composition on the plasma plume dynamics. *Appl. Surf. Sci.* **2017**, *418*, 594–600. [CrossRef]
27. Stoian, R.; Ashkenasi, D.; Rosenfeld, A.; Campbell, E.E.B. Coulomb explosion in ultrashort pulsed laser ablation of Al_2O_3. *Phys. Rev. B* **2000**, *62*, 13167–13173. [CrossRef]
28. Nica, P.; Agop, M.; Gurlui, S.; Focsa, C. Oscillatory Langmuir probe ion current in laser-produced plasma expansion. *EPL* **2010**, *89*, 65001. [CrossRef]
29. Ludmirsky, A.; Givon, M.; Eliezer, S.; Gazit, Y.; Jackel, S.; Krumbein, A.; Szichman, H. Electro-optical measurements of high potentials in laser produced plasmas with fast time resolution. *Laser Part. Beams* **1984**, *2*, 245–250. [CrossRef]
30. Ludmirsky, A.; Eliezer, S.; Arad, B.; Borowitz, A.; Gazit, Y.; Jackel, S.; Krumbein, A.D.; Salzmann, D.; Szichman, H. Experimental Evidence of Charge Separation (Double Layer) in Laser-Produced Plasmas. *IEEE Trans. Plasma Sci.* **1985**, *13*, 132–134. [CrossRef]
31. Irimiciuc, S.A.; Agop, M.; Nica, P.; Gurlui, S.; Mihaileanu, D.; Toma, S.; Focsa, C. Dispersive effects in laser ablation plasmas. *Jpn. J. Appl. Phys.* **2014**, *53*, 116202. [CrossRef]
32. Boulmer-Leborgne, C.; Benzerga, R.; Perrière, J. Nanoparticle Formation by Femtosecond Laser Ablation. *J. Appl. Phys D* **2007**, *40*, 125–140.
33. Babushok, V.I.; DeLucia, F.C.; Gottfried, J.L.; Munson, C.A.; Miziolek, A.W. Double pulse laser ablation and plasma: Laser induced breakdown spectroscopy signal enhancement. *Spectrochim. Acta Part B At. Spectrosc.* **2006**, *61*, 999–1014. [CrossRef]